



HAL
open science

Cooling of a Magmatic System Under Thermal Chaotic Mixing

Kamal El Omari, Yves Le Guer, Diego Perugini, Maurizio Petrelli

► **To cite this version:**

Kamal El Omari, Yves Le Guer, Diego Perugini, Maurizio Petrelli. Cooling of a Magmatic System Under Thermal Chaotic Mixing. *Pure and Applied Geophysics*, 2015, 172 (7), pp.1835-1849. 10.1007/s00024-014-1029-y . hal-02153358

HAL Id: hal-02153358

<https://univ-pau.hal.science/hal-02153358>

Submitted on 23 Oct 2020

HAL is a multi-disciplinary open access archive for the deposit and dissemination of scientific research documents, whether they are published or not. The documents may come from teaching and research institutions in France or abroad, or from public or private research centers.

L'archive ouverte pluridisciplinaire **HAL**, est destinée au dépôt et à la diffusion de documents scientifiques de niveau recherche, publiés ou non, émanant des établissements d'enseignement et de recherche français ou étrangers, des laboratoires publics ou privés.

Cooling of a Magmatic System Under Thermal Chaotic Mixing

KAMAL EL OMARI,¹ YVES LE GUER,¹ DIEGO PERUGINI,² and MAURIZIO PETRELLI²

Abstract—The cooling of a basaltic melt undergoing chaotic advection is studied numerically for a magma with a temperature-dependent viscosity in a two-dimensional (2D) cavity with moving boundary. Different statistical mixing and energy indicators are used to characterize the efficiency of cooling by thermal chaotic mixing. We show that different cooling rates can be obtained during the thermal mixing of a single basaltic magmatic batch undergoing chaotic advection. This process can induce complex temperature patterns inside the magma chamber. The emergence of chaotic dynamics strongly modulates the temperature fields over time and greatly increases the cooling rates. This mechanism has implications for the thermal lifetime of the magmatic body and may favor the appearance of chemical heterogeneities in the igneous system as a result of different crystallization rates. Results from this study also highlight that even a single magma batch can develop, under chaotic thermal advection, complex thermal and therefore compositional patterns resulting from different cooling rates, which can account for some natural features that, to date, have received unsatisfactory explanations, including the production of magmatic enclaves showing completely different cooling histories compared with the host magma, compositional zoning in mineral phases, and the generation of large-scale compositional zoning observed in many plutons worldwide.

Key words: Magma cooling, chaotic advection, thermal lifetime of magma chambers, temperature-dependent viscosity, crystallinity, thermal eigenmodes, numerical simulation.

List of symbols

A	Area (m ²)
C_p	Heat capacity (J/kgK)
k	Thermal conductivity (W/mK)
L	Wall characteristic length (m)

Dimensionless numbers

Nu	Nusselt number
----	----------------

Φ	Crystal fraction
Pr	Prandtl number
Re	Reynolds number
T^*	Dimensionless temperature
X	Rescaled dimensionless temperature

Greek symbols

ρ	Fluid density (kg/m ³)
σ	Standard deviation
τ	Period of modulation (s)

Subscript

m	Mean
---	------

1. Introduction

Thermal equilibrium is of great interest in both petrology and volcanology because the possible evolution of magmatic systems strongly depends on the development of thermal and compositional heterogeneities which, in turn, can influence the capability of the magmatic mass to differentiate and/or erupt. It has recently been shown that magmatic systems can exhibit wide compositional heterogeneity in both space and time (e.g., PERUGINI and POLI 2012; PERUGINI *et al.* 2012). This heterogeneity is the result of complex processes developing in magmatic masses and is mostly considered to be a result of chaotic dynamics (i.e., magma mixing; DE CAMPOS 2011; MORGAVI *et al.* 2013; PERUGINI *et al.* 2012). The presence of chaotic behaviors in igneous systems is widely reported in literature (e.g., BERGANTZ 2000; PETRELLI *et al.* 2011; PERUGINI and POLI 2012; PERUGINI *et al.* 2012), but surprisingly, there are few contributions addressing the thermal behavior of a magmatic body experiencing chaotic dynamics. Since the late 1990s, different works on thermal advection of

¹ Laboratoire SIAME, Fédération CNRS IPRA, Université de Pau et des Pays de l'Adour (UPPA), 64000 Pau, France. E-mail: kamal.elomari@univ-pau.fr; yves.leguer@univ-pau.fr

² Department of Physics and Geology, University of Perugia, Perugia, Italy. E-mail: diego.perugini@unipg.it; maurizio.petrelli@unipg.it

high-viscosity fluids have shown that temperature fields can be strongly modulated by the onset of chaotic dynamics (SAATDJIAN and LEPREVOST 1998; LEFEVRE *et al.* 2003; MOTA *et al.* 2007; EL OMARI and LE GUER 2010a; LE GUER and EL OMARI 2012), but they are mostly confined to industrial processes. Therefore, study of the thermal evolution of a magmatic body in a chaotic environment could be of great interest and would start to fill the gap in previous and recent literature. The development of different thermal domains in space and time may, in fact, strongly influence the cooling history of the magmatic mass and therefore crystallization, leading to the formation of volumes of melts with strong rheological and compositional differences. As an example, crystal-size distributions have long been known to be influenced by the cooling kinetics of the magma (WINKLER 1949). Different cooling histories may also induce differential rates of growth for crystals. In this work, we focus on the cooling kinetics of a batch of magmatic melt undergoing very low advection. In particular, we present numerical simulations of chaotic thermal advection aimed at understanding the space and time modulation of the temperature field during cooling of a mafic melt. The temperature dependence of the magma viscosity is taken into account. Results are discussed in the light of the timescales of cooling for the magmatic body and the impact of this process on the evolution of the magmatic mass. The production of different thermal domains in which magma crystallization may proceed with differential efficiency is also discussed.

2. The Physical Problem

2.1. Conceptual Model and Properties of the Mafic Magma

The study of several natural magmatic systems has repeatedly led to the inference that the magma dynamics are governed by chaotic dynamics (e.g., FLINDERS and CLEMENS 1996; DE ROSA *et al.* 2002; PERUGINI *et al.* 2003, 2006). The fact that magma dynamics is chaotic means that its investigation can be reduced, as a first approximation, to the study of

stretching and folding of the silicate melt. This approach has enabled the investigation of the interplay between flow fields and the modulation of geochemical composition in the magmatic system (e.g., PERUGINI *et al.* 2003, 2006). Despite the simplicity of such an approach, it is important to note that it is capable of generating structures and compositional patterns that mimic those observed in natural rocks (e.g., PERUGINI *et al.* 2003; PERUGINI and POLI 2012). This observation confirms that a system exhibiting chaotic advection contains much that is necessary for replicating the fluid-dynamic evolution of a magma body. Thus, irrespective of the specific processes responsible for advection (e.g., convection, flow in conduits, etc.), chaotic dynamics of magmas is a very powerful conceptual tool for addressing the complexity of this petrogenetic and volcanological process. Guided by this conceptual model, we consider here the thermal chaotic mixing in a 2D rectangular cavity filled with a Newtonian mafic magma (Fig. 1). The numerical system contains all essential ingredients and fundamental building blocks to replicate the basic fluid dynamics of a magma body, consisting of stretching and folding processes. We consider that the cavity is not open to mass fluxes, implying that, once in place, the mafic batch behaves as a closed system. The thermophysical properties of the mafic magma are given in Table 1. The initial temperature T_i of the molten magma is chosen as $1,200\text{ }^\circ\text{C}$ (liquidus temperature), and the

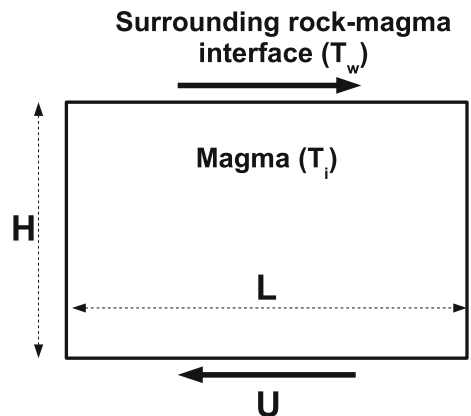


Figure 1

Sketch of the two-dimensional magma chamber (aspect ratio 0.6)

Table 1

Thermophysical properties of the melted mafic magma at the initial temperature T_i

Mafic magma property	Value	Unit
Density, ρ	2,750	kg m ⁻³
Thermal conductivity, k	2.2	W m ⁻¹ K ⁻¹
Thermal diffusivity, α	8×10^{-7}	m ² s ⁻¹
Specific heat, C_p	1,000	J kg ⁻¹ K ⁻¹
Dynamic viscosity, μ ($T_i = 1,200$ °C)	100	Pa s

temperature of the surrounding rock–magma interface T_w is 600 °C. All the thermophysical properties are considered independent of temperature except the viscosity, as explained in the following section. The corresponding Prandtl number at the initial temperature of the magma is $Pr = 45,450$. For this high Prandtl number, the magma flow is characterized by a flow momentum much higher than the heat diffusion. Classically, for a steady laminar flow, the wall effects will be felt further inside the magma chamber for the velocity field than for the thermal field, thus the magma cooling will be governed by what happens in the vicinity of the walls (EL OMARI and LE GUER 2010). We will see that this mechanism will differ when chaotic advection enters into action. We limit the study to magmas at the early stages of crystallization, and we assume that no release of latent heat of crystallization occurs during the formation of crystals (see Sect. 2.2). The crystallization is envisaged as a phenomenon directly linked to the increases in the viscosity of the melt during cooling. Although these assumptions might appear quite severe, as reported in the introductory section, the aim of this study is to investigate the sole effect of chaotic advection on the thermal field to assess the kinetics of cooling of a mafic magma. As another assumption, we consider that the density remains constant during the cooling of the magma. Thus, natural convection due to buoyancy is not possible inside the magma chamber (i.e., convective thermal plumes BRANDEIS and JAUPART 1986). Assuming a constant density within the magma chamber is in keeping with the idea that we study natural magmas at the early stages of the differentiation process, as stated above.

2.2. Magma Viscosity and Viscosity–Crystallinity Relation

Magma viscosity is primarily linked to its silica content. The higher the amount of silica in a magma, the more viscous the magma will be due to the strong silicon–oxygen bonds which produce silica chains. Since we are investigating a mafic magma at the early stages of crystallization (i.e., low chemical variations), we neglect the link of viscosity to chemical composition. The gas content also affects the magma viscosity. We assume that the system contains a fixed amount of gas phases (closed system) and that their content is below the saturation value (i.e., no gaseous exsolution occurs). Other factors that strongly influence magma viscosity are temperature and crystal content. The viscosity increases with decreasing temperature and with increasing crystal content. In this study we consider a pseudo-Newtonian fluid (with no yield stress and a viscosity not dependent on strain rate) for which the temperature dependence of the viscosity is modeled by an exponential law that can simulate the rapid increase in viscosity when tiny crystals form during cooling (MC BIRNEY and MURASE 1984; SPERA 2000; COSTA and MACEDONIO 2003; GIORDANO *et al.* 2008):

$$\mu = \mu_0 \exp(B(1 - T^*)) \quad (1)$$

with μ_0 the viscosity at the initial temperature ($T^* = 1$), here considered equal to 100 Pa s. B is the Pearson number that takes into account the increase of viscosity with cooling (LE GUER and EL OMARI 2012). In this study, three cases are considered: the non-temperature-dependent, reference case ($B = 0$), and cases with moderate ($B = 5$) and greater temperature dependence ($B = 10$). The parameter B determines how fast the viscosity increases as the temperature of the magma is lowered. The viscosity range is from 100 Pa s for the mafic melt at the initial temperature, near its liquidus temperature, to about 10^6 – 10^7 Pa s for the same magma now containing a certain amount of crystals. The assumption that the magma is a Newtonian fluid is valid when we consider temperatures near the liquidus. This fact was confirmed by the measurements of SATO (2005) for the 1707 basalt from Mount Fuji volcano, for which the viscosity is almost constant against shear rate at 1,210 °C,

corresponding to a melt with very low crystal content. As the temperature is lowered (subliquidus temperatures), a non-Newtonian shear thinning might appear depending on several parameters such as the quantity and morphology of crystals (CIMARELLI *et al.* 2011) and the applied strain rate (CARICCHI *et al.* 2007). MADER *et al.* (2013) extensively reviewed the rheology of two-phase magmas, reporting that the rheology of a crystal-bearing igneous system mostly depends on the crystal fraction Φ , the critical crystal fraction at which particles cannot move past one another (i.e., the maximum packing fraction Φ_{cr}), and the flow index n . The latter is a function of the Φ/Φ_{cr} ratio and of the crystal aspect ratio (MADER *et al.* 2013). As reported by MADER *et al.* (2013), a magmatic system is always Newtonian for $\Phi/\Phi_{cr} < 0.5$. For higher values of Φ/Φ_{cr} (i.e., $0.5 < \Phi/\Phi_{cr} < 0.8$), the Newtonian behavior still persists for values of the flow index n equal to or greater than 0.9. The values of Φ_{cr} are not easy to unravel in natural magmatic systems (MADER *et al.* 2013). Using a geometric approach, Φ_{cr} is about 0.74, if crystals are subspherical. The value of Φ_{cr} is lower for disordered systems ($\Phi_{cr} \approx 0.64$; MADER *et al.* 2013). Assuming $\Phi_{cr} = 0.656$ (smooth particles; MADER *et al.* 2013), the behavior of the system can be safely considered to be Newtonian for crystal content Φ up to 0.32. Studying a natural system, MARSH (1981) states that the limit of the phenocrystal content observed in basaltic lavas is $\Phi_{cr} = 0.55$; above this critical point the viscosity of the magma is so high that it cannot erupt as lava. The maximum packing density corresponds to a minimum of liquid content in the melt or equivalently to a minimum of porosity, which is highly dependent on the morphology of the crystals and their polydispersity. The viscosity of the magma also depends intimately on the shape of the crystals and their polydispersity. Moreover, the nucleation and growth rates of these crystals are closely linked to the local cooling rate encountered inside the magma. Magma cooling rates are related to the thermal fields, which are intimately linked to the flow kinematics. To summarize the behavior described by MADER *et al.* (2013), a mafic magma with low crystal content ($\Phi < 30\%$) can be reasonably considered as a Newtonian fluid if the crystal aspect ratio is not larger than 3.2. For higher content of crystals and/or larger

values of the crystal aspect ratio, a rheological transition characterized by a rapid increase of the apparent viscosity occurs. A complete review of the transition from Newtonian to non-Newtonian behavior lies beyond the scope of this work, and to be conservative, we limit the discussion of results to magmatic systems with crystal content below 30% (i.e., $\Phi = 0.3$). Classically, the model given in the literature to link the apparent viscosity to the degree of crystallinity is the Krieger–Dougherty model (KRIEGER and DOUGHERTY 1959) derived from the Einstein–Roscoe model (ROSCOE 1952):

$$\frac{\mu}{\mu_0} = \left(1 - \frac{\Phi}{\Phi_{cr}}\right)^{-\beta}, \quad (2)$$

where Φ_{cr} is the critical volume fraction and the exponent β is a fitting parameter correlated with Φ_{cr} to account for particle shape (CIMARELLI *et al.* 2011). This model is appropriate to fit the data mainly for low crystal concentrations.

2.3. Chaotic Advection Flow

The chaotic advection phenomenon is now well known to enhance fluid mixing, reactive mixing or heat transfer in many industrial processes (AREF 1984; OTTINO 1989). It is also recognized to be of particular importance for natural phenomena in various earth domains such as volcanology (METCALFE *et al.* 1995; PERUGINI and POLI 2012; RENJITH *et al.* 2013), atmospheric sciences or oceanic dispersion (pollutants, black tides or plankton blooms; LOPEZ *et al.* 2001). Chaotic advection becomes particularly interesting for applications where the viscous effects are large compared with inertial effects (i.e., very low Reynolds numbers). This can be encountered for problems which involve small physical dimensions (typically for microfluidic applications), for very low velocities or for very large viscosities. The flow of a magma couples two of these elements (i.e., large viscosity and low velocity of the chamber wall, if present). For two-dimensional chaotic advective flows, a simple unsteady velocity field is able to generate very complex tracer patterns (concentration or temperature fields) (AREF 2002). The global mixing mechanism comprises a stirring phase related to the stretching and folding of fluid

elements (as blobs and filaments) and a mixing phase. By chaotic advection, we mean that nearby fluid elements separate from each other exponentially in time in particular domains of the flow. That is why mixing is greatly enhanced due to the efficient generation of interfaces between scalars, which then facilitates the diffusion of the scalar through these interfaces (the mixing phase itself). It is not necessary for the velocity field itself to be chaotic as in turbulence to obtain chaotic trajectories of particles. A necessary constraint to produce chaotic advection in two-dimensional flow is to break the time invariability of the streamlines, as obtained by considering an unsteady flow with moving magma chamber walls in the present study. The 2D rectangular cavity we have chosen for the study of the magma flow is a classical geometry for chaotic advection (CHIEU *et al.* 1986; JANA *et al.* 1994; LIU *et al.* 1994). It has a height/length ratio (H/L) of 0.6. As a stirring protocol, a constant velocity is imposed alternately on the side walls during each half period (Fig. 2). Thus, a nondimensional period τ controls the efficiency of the thermal mixing. In this study, a highly laminar magmatic flow is chosen with a reference Reynolds number equal to 1 for the simulations. This reference Reynolds number is based on the viscosity of the initial hot magma μ_0 (at $T_i = 1,200$ °C). As the viscosity at the initial temperature of the magma is fixed, the product $U \cdot L$ is constant and the couple (U, L) has to be chosen. Thus, U and L are dependent variables for this problem. For the temperature-dependent viscosity cases, when the magma viscosity increases, the Reynolds number becomes smaller. Thus, a simple shear flow is applied to the magma chamber and the stirring protocols correspond to alternating movement of the two side walls at a given constant velocity, originating chaotic dynamics. As explained above, this protocol has been chosen to trigger chaotic advection in the magmatic system according to natural evidence and previous studies where magma mixing processes have been widely documented (e.g., PERUGINI and POLI 2012; PERUGINI *et al.* 2006, 2007).

The chosen period is one allowing the chamber side walls to be swept alternately five times each ($\tau = 10$). In order to show the time scales involved in the chaotic mixing mechanism for the magmatic

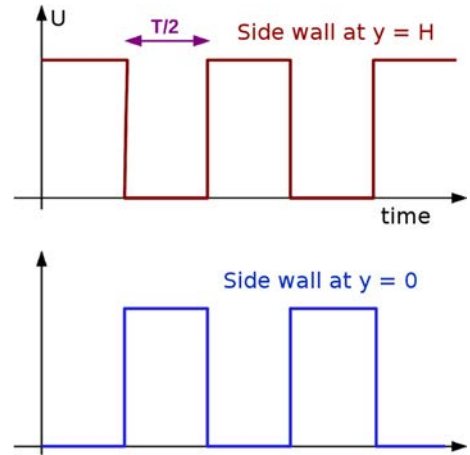


Figure 2
Temporal modulation of the magma chamber walls (stirring protocol)

system, in Table 2, for $Re = 1$, the time unit L/U and the real time of a period of stirring are given for three sizes L of the magma chamber (the associated velocities U are fixed as explained above). As an indication, the operating shear rate in the magmatic body is also given.

In a recent work, EL OMARI and LE GUER (2010a) showed that the global thermal chaotic mixing is very sensitive to the wall kinematics and that the stagnation parabolic points at the wall play a key role. Our objective in this study is also to verify this point for the thermal mixing occurring during the cooling of the magmatic mass.

3. Mathematical Formulation

3.1. Conservation Equations and Flow Parameters

The governing equations (Navier–Stokes, energy, and continuity) are solved for the 2D cavity described above. Some hypotheses are considered: gravity is considered normal to the cavity plane, thus no natural convective flow can develop inside the cavity as the density is not dependent on the temperature as indicated in the Sect. 1; additionally no viscous heating effect is considered. This last assumption is justified even with the consideration of the exponential increase of the viscosity with temperature because the velocities considered are very low; the Brinkman number (Br) which characterizes the

Table 2

Time unit and real time associated to a period of stirring for Reynolds number equal to 1 and different sizes of magma chamber

Re = 1	Time unit L/U	Real time for a period $10 L/U$	Shear rate
$L = 100$ m			
$U = 3.63 \times 10^{-4}$ m s ⁻¹	3.19 days	≈32 days	≈10 ⁻⁵ s ⁻¹
$L = 1,000$ m			
$U = 3.63 \times 10^{-5}$ m s ⁻¹	0.87 years	≈8.72 years	≈10 ⁻⁷ s ⁻¹
$L = 10,000$ m			
$U = 3.63 \times 10^{-6}$ m s ⁻¹	87.2 years	≈872 years	≈10 ⁻⁹ s ⁻¹

The corresponding initial shear rate is also given

relative importance of the viscous dissipation in the energy equation is very low:

$$\text{Br} = \frac{\mu_0 \cdot U^2}{k \cdot (T_i - T_w)} \ll 1. \quad (3)$$

Thus, the viscous heating term is neglected in the energy equation (LE GUER and EL OMARI 2012). Additional nonlinearities are introduced into the problem via the viscosity law, which is taken to depend on temperature, and also through the inclusion of inertia. Considering the parameter values given in Table 2, the Strouhal number is around 0.1, which is not too small. As a consequence, the flow does not satisfy the quasisteady hypothesis and the acceleration and deceleration phases imposed on the walls will influence the mixing inside the whole cavity.

The unsteady convective heat transfer cooling problem is governed by the nondimensional conservation equations for mass, momentum, and energy:

$$\nabla \cdot \mathbf{v} = 0, \quad (4)$$

$$\partial_t \mathbf{v} + (\mathbf{v} \cdot \nabla) \mathbf{v} = -\nabla \mathbf{p} + \frac{1}{\text{Re}} \nabla \cdot \left(\frac{\mu}{\mu_0} (\nabla \mathbf{v} + (\nabla \mathbf{v})^T) \right), \quad (5)$$

$$\partial_t T^* + \mathbf{v} \cdot \nabla T^* = \frac{1}{\text{RePr}} \nabla^2 T^*, \quad (6)$$

where

$$\text{Re} = \frac{\rho UL}{\mu_0}, \quad \text{Pr} = \frac{\mu_0 C_p}{k}, \quad \text{and } T^* = \frac{T - T_w}{T_i - T_w}$$

The characteristic scales considered for this nondimensional problem are the cavity length L , the

velocity of the wall U , the time U/L , and the pressure ρU^2 . With the above definition of the dimensionless temperature, the maximum temperature difference between the walls and the fluid is always 1. $T^* = 1$ corresponds to the beginning of the thermal mixing (all the magma is at 1,200 °C), and $T^* = 0$ to the magma at the rock temperature of 600 °C. Thus, the 2D unsteady convective heat transfer cooling problem is governed by only two nondimensional numbers (Re and Pr). Another point has to be mentioned, concerning the latent heat of crystallization that is released into the mafic magma during its cooling. For the mafic magma with 30 % of mass fraction crystallized (corresponding to the high viscosity encountered for the low temperatures), we have estimated the Stefan number (characterizing the ratio of sensible heat to latent heat) to be above 20. This high ratio indicates that, as a first approximation, the latent heat of crystallization can be neglected, despite the role it may play in localized areas near solidification fronts.

3.2. Numerical Method

The continuity and Navier–Stokes equations were solved, as well as the energy conservation equation, by means of an in-house code (Tamaris) based on the unstructured finite-volume method. Spatial schemes approximating convective and diffusive fluxes are second-order accurate. The convective fluxes are approximated by the high-resolution nonlinear CUBISTA scheme in order to reduce the numerical diffusion. This is crucial to avoid overshoot of the thermal diffusion in the energy equation. Time advancement is ensured by the implicit, second-order-accurate, three-time-step Gear scheme, while the pressure and velocity fields are coupled by the SIMPLE algorithm. A parallel algebraic multigrid (AMG) solver is used to resolve the obtained linear systems, since a sufficiently fine mesh of 54,000 computational cells was used to capture possible striations arising in the temperature field. This mesh was chosen after a thorough study of the dependence of the results on mesh size. The MCIA supercomputer at Bordeaux was used for the parallel calculations. More details about the numerical methods used and code validations are given elsewhere

(EL OMARI and LE GUER 2009, 2010a, b, 2012; BAMMOU *et al.* 2013).

3.3. Thermal Mixing Indicators

We mainly use three statistical mixing indicators to characterize the efficiency of heat transfer by chaotic thermal mixing: the mean temperature, the variance, and the Nusselt number. Their evolutions are followed over time during the magma cooling. The mean temperature of the magma T_m^* , which represents the energy extracted from the fluid across the walls (EL OMARI and LE GUER 2010), is given by

$$T_m^* = \frac{1}{\sum_c A_c} \left(\sum_c A_c T_c^* \right), \quad (7)$$

where the summation is made over all 2D computational cells of area A_c (the subscript c is for cell). Indeed, the mean temperature evolution can be seen as an indicator of the ratio of the total energy supplied to the fluid from the initial time considered to the time t :

$$E(t) = \rho C_p V_{chamber} (T_m(t) - T_w). \quad (8)$$

Hence, the mean temperature is asymptotically bounded by the fixed temperature imposed on the walls (i.e., T_w or $T_m^* = 0$ for nondimensional temperature). The second indicator is the variance σ^2 of the fluid temperature, which represents the level of homogenization of the scalar temperature inside the 2D magma chamber (STREMLER 2008):

$$\sigma^2 = \frac{1}{\sum_c A_c} \sum_c \left(A_c (T_c^* - T_m^*)^2 \right). \quad (9)$$

For a thermal mixing problem without any source of scalar, the advection–diffusion equation indicates that the temperature fluctuations evolve towards a uniform state ($\sigma^2 = 0$) at a decay rate given by the product of twice the thermal diffusivity α and the temperature gradients induced by the flow inside the magma chamber (THIFFEAULT 2012). Thus, for our case, as the thermal diffusivity is given and the flow field chosen, the speed at which the magma will be cooled will be studied by following the decay rate of σ^2 over time for different temperature-dependent viscosity cases. The last indicator used is the mean

Nusselt number \overline{Nu} , which characterizes the strength of heat transfer across a wall. It represents the dimensionless temperature gradient in a direction normal to the wall:

$$\overline{Nu} = \frac{1}{S_w} \int_{S_w} \nabla \mathbf{T}^* \cdot \mathbf{n} \, d\mathbf{S}. \quad (10)$$

Since we consider here that the wall temperature (the temperature of the surrounding rock–magma interface) is kept constant during the cooling, the parietal heat flux exhibits a nonuniform distribution along the boundaries of the chamber (i.e., a nonuniform temperature gradient distribution). This distribution is closely related to the complex fluid flow kinematics inside the magma chamber.

4. Results and Discussion

4.1. Flow Streamlines, Temperature, and Crystallinity Field Patterns

In Fig. 3, one can observe the streamlines in the cavity flow system corresponding to the separate motion of each wall for the non-temperature-dependent viscosity case. Despite their simplicity, the combination of these two very simple Eulerian velocity fields produces very complex irregular Lagrangian trajectories that consequently give complex temperature patterns, as shown in Fig. 4, which presents several snapshots of the temperature field taken at different periodic times for two values of the Pearson number \mathbf{B} . We observe highly elongated and folded striations produced by chaotic advection near the rock walls of the magma chamber, with cold magma tongues penetrating inside the chamber; these structures lead to the existence of flow regions with very different temperature levels. For the case $B = 0$, one can notice the existence of a large unmixed thermal zone in the central part of the domain with two filaments emanating from it which move together in the magmatic chamber during chaotic advection. This island of hot magma is transported across the magma chamber without shape distortion, undergoing weaker cooling compared with parietal areas (BRESLER 1997). After a transient stage, the spatial

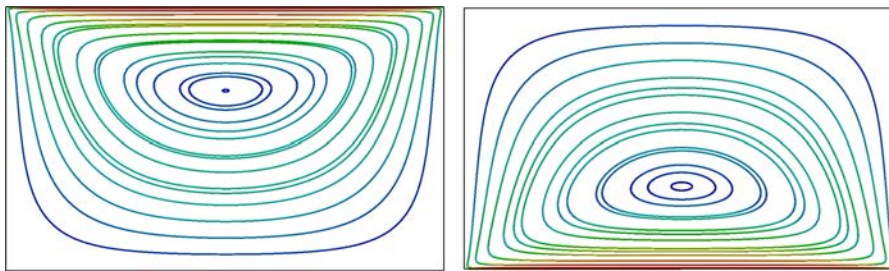


Figure 3

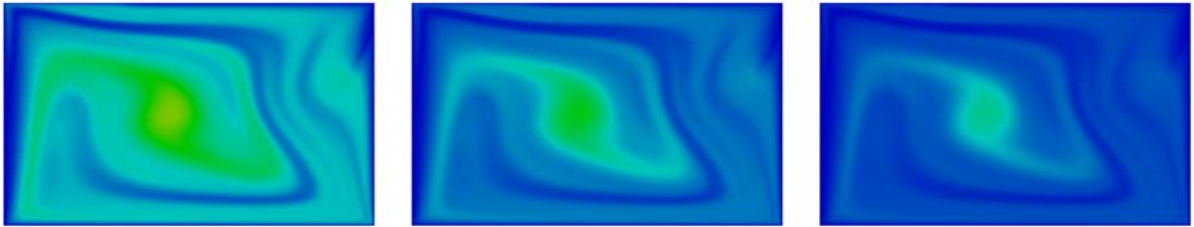
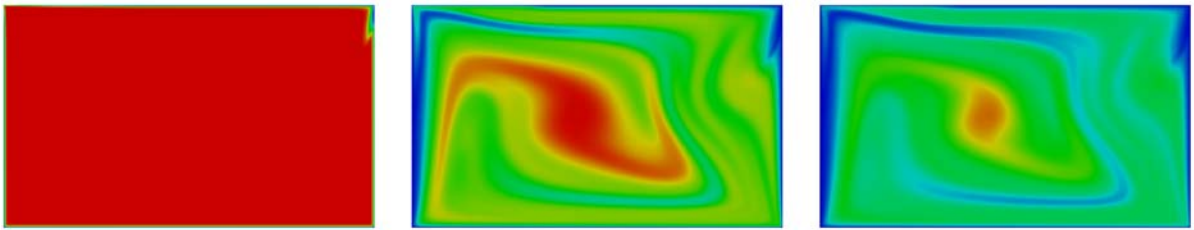
Flow streamlines induced by the wall movements during the first (*left*) and second (*right*) half-period of the stirring protocol

distribution of the temperature patterns takes the same form at each periodic time but the amplitude of the dimensionless temperature differences tends towards 0; these self-similar structures are called thermal strange eigenmodes (EL OMARI and LE GUER 2010; LIU and HALLER 2004) and are the signature of an underlying fractal structure in the flow. The spatial structure of the temperature field is smooth; this is due to the relatively high value of the thermal diffusivity and is also the reason why only relatively large temperature striations are observed. By comparison, the spatial structures of the concentration patterns would have presented more lamellar structures due to the lower value of the molecular diffusivity. The thermal diffusion blurs the fine-scale structure of the representative thermal strange eigenmode. The direct consequence of the existence of this thermal strange eigenmode is that the crystallization front in such a chaotic flow will not last long parallel to the walls, as classically considered for the cooling of a magmatic chamber (HUPPERT 2000). The result could be the existence of a magmatic enclave, which would appear after complete solidification of the magmatic mass (e.g., DIDIER and BARBARIN 1999; PERUGINI and POLI 2000). This process could also account for the widespread occurrence of compositional zoning in mineral phases (e.g., GINIBRE *et al.* 2002; PERUGINI *et al.* 2005). In fact, as minerals are transferred among the different dynamic regions, they can undergo multiple episodes of resorption and growth according to the thermal and compositional features of the different regions existing within the magmatic system. At larger length scales, this could also generate compositional zoning in the magmatic mass, as observed in several plutons worldwide (e.g.,

MAHOOD and FRIDRICH 1982; HECHT and VIGNERESSE 1999). The effect of temperature-dependent viscosity is noticeable, since these hot zones disappear for $B = 5$. This is due to the strong increase of the magma viscosity in the vicinity of the cold walls, which promotes the carriage of magmatic liquid by the moving walls and thus improves the stirring. The period that corresponds to the establishment of a persistent temperature pattern seems to be much longer than before for the case $B = 0$. The self-similar patterns also seem to appear much later. This fact is confirmed below by observations of the probability distribution functions (PDFs) of temperature. The case with greater temperature dependence ($B = 10$) is illustrated in Fig. 5. The strong effect of the temperature-dependent viscosity on the velocity field is clearly shown in the evolution of the streamlines. At $t = 5\tau$, for example, the streamlines are deformed and a small new vortex appears in a corner of the magma chamber. The temperature patterns are correlatively modified: they do not align with the streamlines and are, in some regions of the chamber, perpendicular to them. A complex spatial distribution of the temperature gradients over the whole domain is thus obtained.

In Fig. 6, the crystallinity fields are plotted for the case $B = 5$ using the Krieger–Dougherty model. We recall that this model is appropriate for low crystal fractions up to the critical value of $\Phi_{cr} = 0.4$ (MADER *et al.* 2013). Starting with zero crystallinity at the first instant (all the magma is at the liquidus temperature), the crystallinity rapidly reaches values around 0.3 in some convoluted zones of the cavity. These zones correspond exactly to the cold zones in the temperature patterns of Fig. 4 (for $B = 5$). High degrees of

Non temperature-dependent viscosity case ($B=0$)



Temperature-dependent viscosity case ($B=5$)

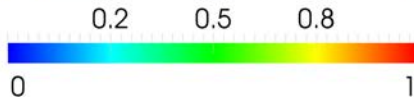
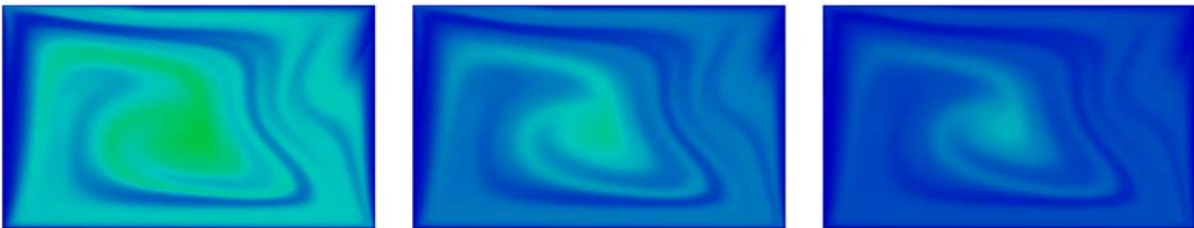
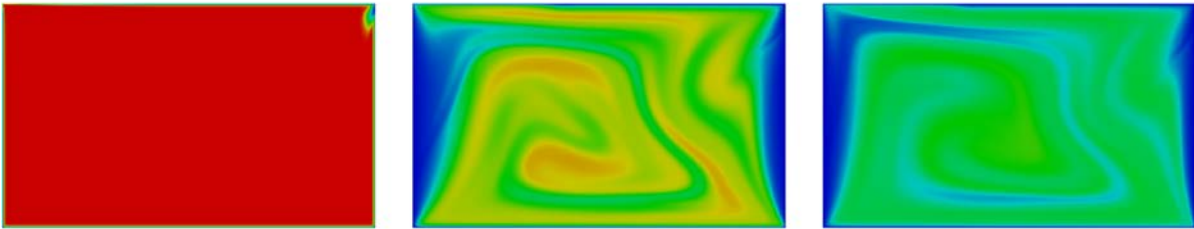


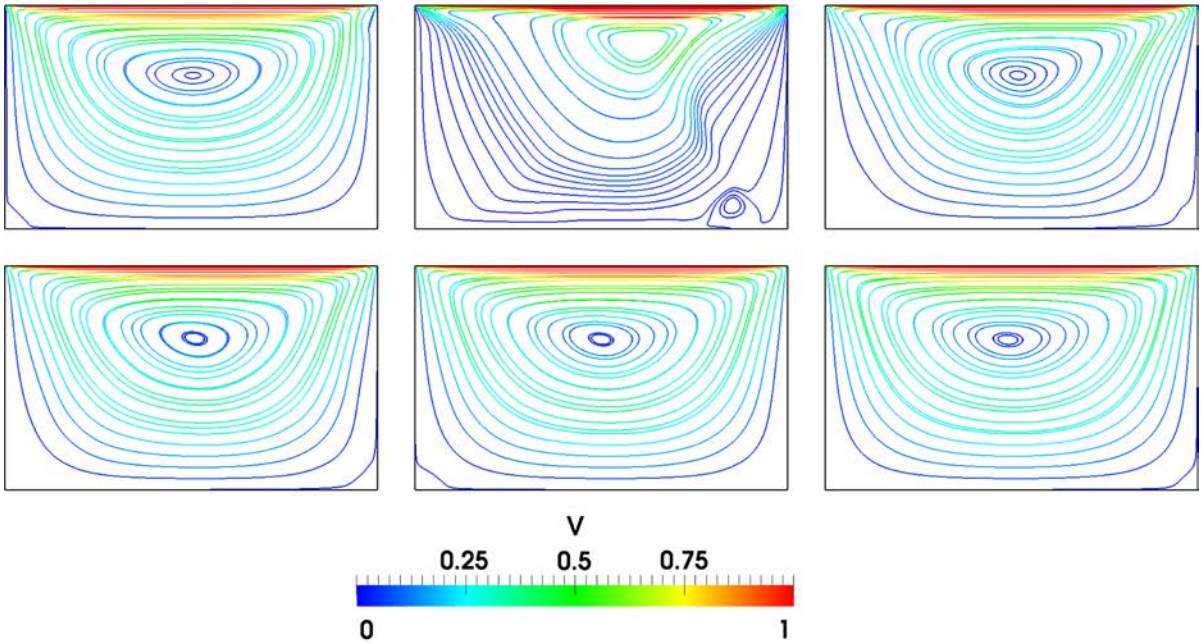
Figure 4

Temperature fields at different periodic instants $t = 0, 5\tau, 10\tau, 15\tau, 20\tau,$ and 25τ (from left to right and top to bottom), for $B = 0$ and 5

crystallinity are thus observable deep inside the magma chamber (for $t = 5\tau$ and 10τ), allowing the formation of solid enclaves that could travel inside the cavity. Thus, the solidification fronts will not develop parallel to the walls. From $t = 20\tau$, the crystallinity becomes almost homogeneous in the cavity around the value 0.3, close to the critical crystallinity for Newtonian behavior.

4.2. Statistical Indicator Evolutions

The impact of the temperature dependence of viscosity on the mixing of magma can be appreciated in the above-mentioned global statistical indicators. In Fig. 7, one can observe the evolution of the mean temperature T_m^* inside the magmatic chamber over



Temperature-dependent viscosity case ($B=10$)

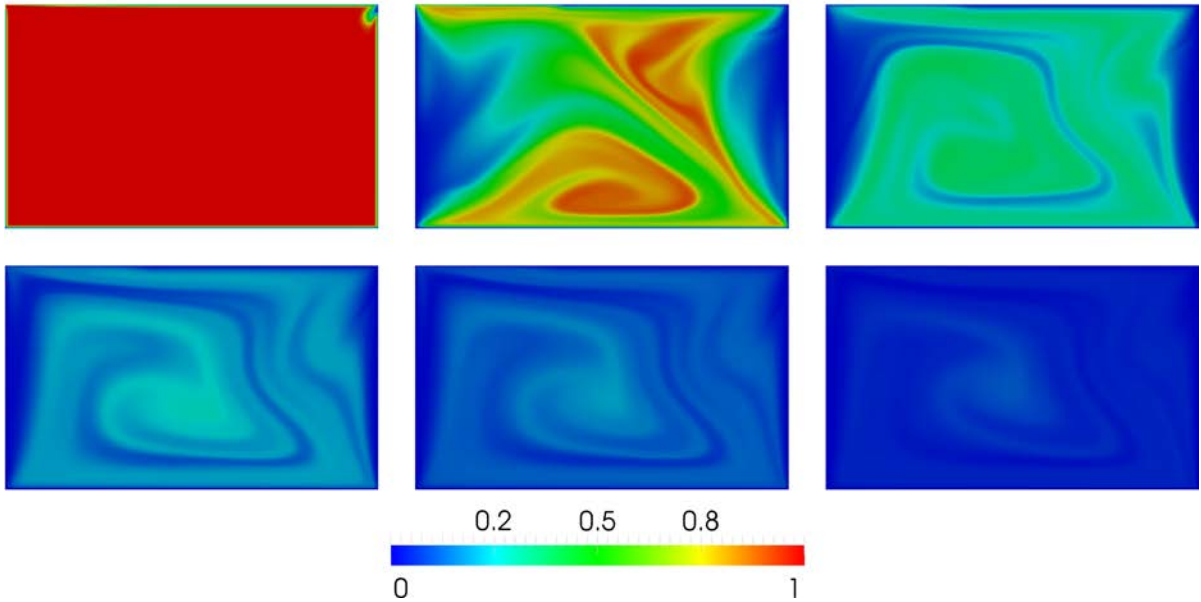


Figure 5

Flow streamlines and temperature fields at different periodic instants $t = 0, 5\tau, 10\tau, 15\tau, 20\tau,$ and 25τ (from left to right and top to bottom), for $B = 10$

time (number of periods) for the three different mixing cases ($B = 0, B = 5,$ and $B = 10$). This represents the amount of energy extracted from the magma across the walls from time 0 to time t . This

figure shows that the mean temperature decreases exponentially towards the wall temperature $T^* = 0$ when chaotic mixing is present ($B = 0$ to $B = 10$ cases), and much more rapidly when the viscosity is

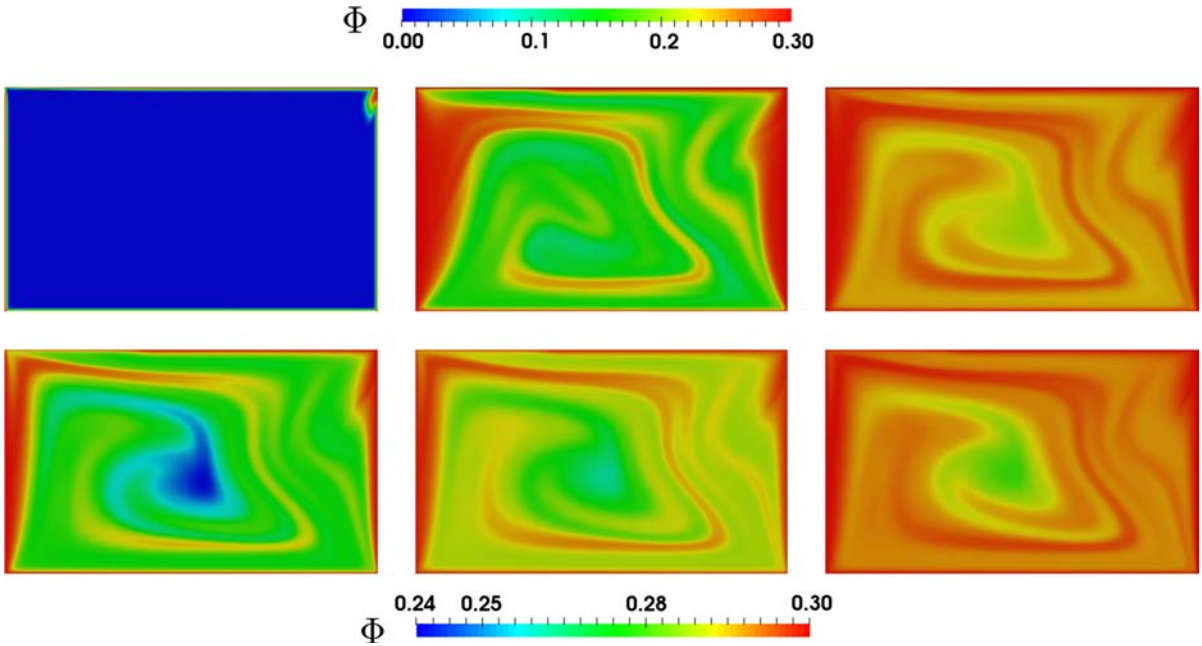


Figure 6

Crystallinity fields at different periodic instants $t = 0, 5\tau, 10\tau, 15\tau, 20\tau,$ and 25τ (from left to right and top to bottom), for $B = 5$ (in relation with the temperature fields of Fig. 4). The color scale is different for top and bottom rows

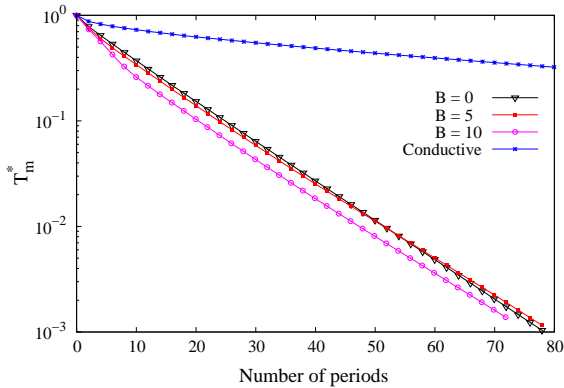


Figure 7

Evolution of the mean temperature for different values of the temperature-dependent viscosity coefficient \mathbf{B} . Comparison with the purely conductive case

high (higher \mathbf{B} value). However, the final decay rates are identical. The purely conductive case (fixed walls) is also given for reference; the slow nature of the thermal mixing is evident, since it operates only by thermal diffusion. This case is also characterized by a temperature field with isotherms parallel to the magma chamber walls.

The standard deviation evolutions are given in Fig. 8 for the same cases. We recall that the variance σ^2 represents the level of homogenization of the temperature inside the magma chamber. We observe first of all a phase which corresponds to the creation of the temperature gradients. This phase is much longer (up to five periods) and the gradient more pronounced when \mathbf{B} is higher. After this transient time, the smoothing of the temperature gradients is observed, being most important for the case $B = 10$. For longer times (after 50 periods), the evolutions are quite similar, with the same decay rate for $B = 0$ and $B = 10$. For the purely conductive case, the temperature homogenization across the magma chamber is very low. This once more confirms the cooling efficiency during chaotic mixing.

Figure 9 illustrates the parietal heat transfer along one of the moving walls. It is characterized by the mean Nusselt number evolution with time, which is found to be globally exponential. The large oscillations of the Nusselt values observed for the three cases are due to the variation of the temperature gradients along the wall resulting from the periodic modulation of the wall movement. For $B = 10$, the

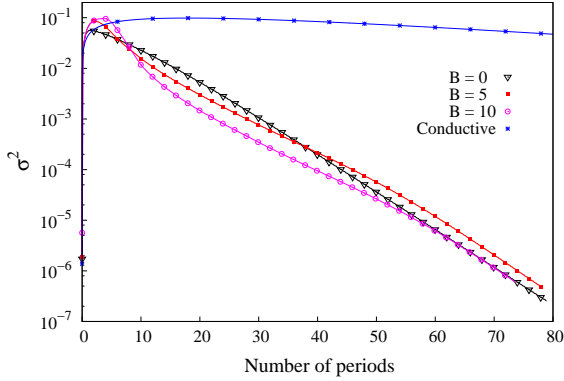


Figure 8

Evolution of the variance for different values of the temperature-dependent viscosity coefficient B . Comparison with the purely conductive case

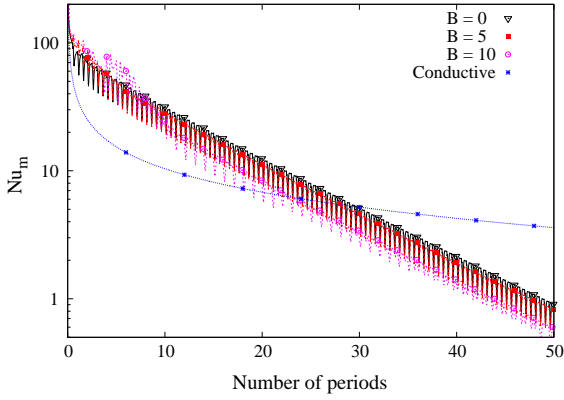


Figure 9

Evolution of the mean Nusselt number along one side wall for different values of the temperature-dependent coefficient B and for the purely conductive case

strong nonlinearity introduced by the temperature-dependent viscosity results in significant irregular fluctuations in the evolution of the Nusselt number.

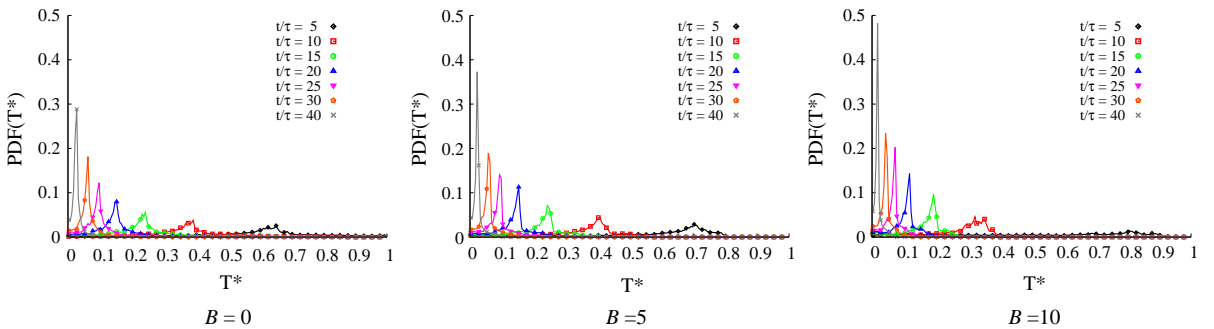


Figure 10

PDFs of the temperature T^* at seven different periodic times for $B = 0$, $B = 5$, and $B = 10$

Without chaotic advection inside the magma chamber (the conductive case), the heat transfer displays a significant slowdown over time. The asymptotical behavior of the Nusselt number evolution in this case is due to the very low penetration of the temperature gradient zone inside the magma chamber.

4.3. Temperature Probability Distribution Functions and Recurrent Patterns

The temperature distributions inside the magma chamber are analyzed by displaying the probability distribution functions (PDFs) of the temperatures at seven different periodic times during the cooling for the cases $B = 0$, $B = 5$, and $B = 10$. At first all the temperatures were $T^* = 1$. When chaotic advection starts, a distribution of temperature appears and a peak is observed, revealing the most represented temperature. This peak moves in time to the left while its height increases. The shift of the PDF towards the left illustrates that the hot temperatures disappear during the thermal mixing process. A narrower distribution is obtained when the mean temperature approaches the wall temperature $T^* = 0$. This effect is much more pronounced for the case $B = 10$, for which the right tail of the distribution is shorter.

An important feature of this thermal chaotic flow is revealed by the PDFs of the rescaled dimensionless temperature X , defined as

$$X = \frac{T^* - T_m^*}{\sigma}. \quad (11)$$

When the dimensionless temperature difference is rescaled by the standard deviation σ , we observe, for $B = 0$, that the distribution for the last periods (from

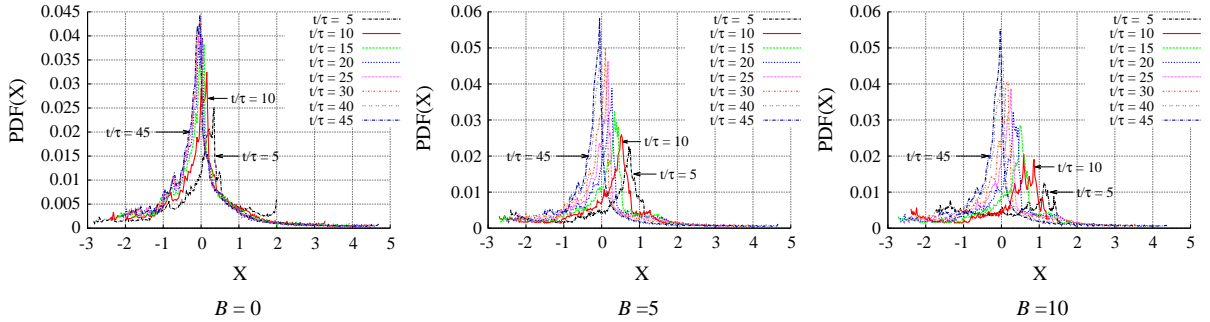


Figure 11
PDFs of the rescaled dimensionless temperature X at seven different periodic times for $B = 0$, $B = 5$, and $B = 10$

$t/\tau = 20$ to $t/\tau = 45$) superimpose (Fig. 11). The superimposed PDFs, plotted for different times during the mixing process but at the same phase of the period, characterize the self-similarity of the dissipation mechanism and are the signature of the existence of a thermal strange eigenmode in the periodic magmatic flow. This is characterized by the production of persistent patterns in the magmatic flow that develop after a transient time (see Fig. 4). These patterns arise from a subtle combination of stretching, folding, and thermal diffusion as the flow is periodically exactly the same (ROTHSTEIN *et al.* 1999; PIKOVSKY and POPOVYCH 2003; LIU and HALLER 2004; EL OMARI and LE GUER 2010). The convergence to the thermal strange eigenmode is also associated with the exponential decay of the dimensionless temperature variance (see Fig. 8). With the increase in the temperature dependence and the nonlinearity due to the stronger link between the velocity field (which is not that of Fig. 3) and the temperature field ($B = 5$ and $B = 10$ cases), the temperature patterns lose their self-similarity and the flow becomes more complex.

5. Conclusions

In this study we investigated the effects of chaotic advection for thermal mixing during the cooling of a mafic magma with temperature-dependent viscosity. The implications for magmatic systems are important. One of the most significant is related to the thermal lifetime of magma chambers. We have shown that, when the thermal field of a magma chamber is governed by chaotic dynamics, it

develops complex structures that are strongly modulated by advective flow fields. This generates different thermal domains due to different cooling efficiencies depending on the ability of chaotic thermal mixing to homogenize the thermal fields; in some cases poorly mixed regions may remain. These correspond to volumes of melt in which heat is transferred with strongly different efficiencies to the surrounding volumes of melt. In strongly stretching regions, heat transfer is fast because of the formation of large contact interfaces. Due to higher heat transfer rates, these regions cool faster than weakly stretching regions, allowing the preservation of chemical structures. This is particularly true for closed systems (i.e., magma chambers that are not refilled by new magma), where the total energy of the system is equal to the initial energy of the system. On the contrary, open systems (e.g., magma chambers continuously refilled by new hot magma) will be able to mix more deeply as a result of the prolonged energy input to the system. In weakly stretching regions, heat dissipation is slower than in strongly stretching areas, because it occurs mainly via diffusion. This allows for the formation of volumes of melt that can potentially preserve the initial temperature for a longer time. Here, chemical homogenization is also very slow due to lower values of chemical diffusion coefficients with respect to thermal diffusion coefficients. As a result, after the beginning of chaotic advection, the magmatic system quickly evolves towards a configuration in which different thermal domains exist. The development of chaotic thermal mixing also contributes to an increase in the space and time complexity of the magmatic system. Moreover, we

have shown that the temperature-dependent viscosity effect is manifested by the introduction of additional complexity in the flow; it also destroys the self-similar character of the temperature fields. This first study was made with the consideration of a certain number of assumptions about the physical phenomena involved. To get closer to a more appropriate magma behavior, consideration of further physical processes could be investigated by numerical simulations for the magma flow, for example, the buoyancy effect if the shear has a component parallel to the gravity field (differentiation), the viscous heating generated by viscous friction near the walls, the non-Newtonian shear-thinning rheological behavior of the magma with or without the existence of a yield stress, and the crystallization kinetics during cooling (including a physical model of magma solidification).

Acknowledgments

We wish to acknowledge the European Research Council for Consolidator Grant CHRONOS (No. 612776) and PRIN no. 2010TT22SC_004 (D.P.). The authors were granted access to the HPC resources of MCIA Bordeaux (France).

Appendix: Supplementary Material

Supplementary material (videos) related to this article can be found online at:

<http://siame.univ-pau.fr/live/transport-multiphasique/Galerie/magma-mixing>.

REFERENCES

- AREF, H. (1984), *Stirring by chaotic advection*, *J. Fluid Mech.* **143**, 1–21.
- AREF, H. (2002), *The development of chaotic advection*. *Phys. Fluids* **2002**, *14*, 1315.
- BAMMOU, L., EL OMARI, K., BLANCHER, S., LE GUER, Y., BENHAMOU, B., MEDIUMI, T. (2013), *A numerical study of the longitudinal thermoconvective rolls in a mixed convection flow in a horizontal channel with a free surface*, *Int. J. Heat Fluid Flow*, **42**, 265–277.
- BERGANTZ, G.W. (2000), *On the dynamics of magma mixing by reintrusion: Implications for pluton assembly processes*, *Journal of Structural Geology*, **22**(9), 1297–1309.
- BRANDEIS, G. and JAUPART, C. (1986), *On the interaction between convection and crystallization in cooling magma chambers*, *Earth and Planetary Science Letters*, **84**, 345–361.
- BRESLER, L., SHINBROT, T., METCALFE, G., OTTINO, J.M. (1997), *Isolated mixing regions: origin, robustness and control*, *Chem. Eng. Sci.* **52**, 1623–1636.
- CARICCHI, L., BURLINI, L., ULMER, P., GERYA, T., VASSALLI, M., PAPALE, P. (2007), *Non-Newtonian rheology of crystal-bearing magmas and implications for magma ascent dynamics*, *Earth and Planetary Science Letters*, **264**(3–4), 402–419.
- CHIEN, W.L., RISING, H., and OTTINO, J.M. (1986), *Laminar mixing and chaotic mixing in several cavity flows*, *J. Fluid Mech.*, **170**, 355, 1986.
- CIMARELLI, C., COSTA, A., MUELLER, S., MADER, H.M. (2011), *Rheology of magmas with bimodal crystal size and shape distributions: Insights from analog experiments*, *Geochemistry, Geophysics, Geosystems*, **12**(7), Q07024.
- COSTA, A. and MACEDONIO, G. (2003), *Viscous heating in fluids with temperature-dependent viscosity: implications for magma flows*, *Nonlin. Processes Geophys.*, **10**, 545–555.
- DE CAMPOS C.P., PERUGINI D., ERTEL-INGRISCH, W., DINGWELL, D.B. and POLI, G. (2011), *Enhancement of magma mixing efficiency by chaotic dynamics: an experimental study*, *Contributions to Mineralogy and Petrology*, **161**, 863–881.
- DE ROSA, R., DONATO, P. and VENTURA, G. (2002), *Fractal analysis of mingled/mixed magmas: an example from the Upper Pollara eruption (Salina Island, southern Tyrrhenian Sea, Italy)*, *Lithos*, **65**, 299–311.
- DIDIER, J., and BARBARIN, B. (1999), *Enclaves and Granite Petrology*, *Developments in Petrology*, **13**, (Elsevier, Amsterdam), 625 pp.
- EL OMARI, K. and LE GUER, Y. (2009), *A numerical study of thermal chaotic mixing in a two rod rotating mixer*, *Computational Thermal Sciences*, **1**, 55–73.
- EL OMARI, K. and LE GUER, Y. (2010a), *Alternate rotating walls for thermal chaotic mixing*. *Int. J. of Heat and Mass Transfer*, **53**, 123–134.
- EL OMARI, K. and LE GUER, Y. (2010b), *Thermal chaotic mixing of power law fluids in an alternate rotating walls mixer*, *Int. J. Non-Newtonian Fluid Mech.*, **165**, 11–12, 641–651.
- EL OMARI, K. and LE GUER, Y. (2012), *Laminar mixing and heat transfer for constant heat flux boundary condition*, *Heat and Mass Transfer*, **48**(8), 1285–1296.
- FLINDERS, J. and CLEMENS, J.D. (1996), *Non-linear dynamics, chaos, complexity and enclaves in granitoid magmas*, *Trans. R. Soc. Edinburgh Earth Sci.* **87**, 225–232.
- GINIBRE, C., KRONZ, A. and WORNER, G. (2002), *High-resolution quantitative imaging of plagioclase composition using accumulated back-scattered electron images: New constraints on oscillatory zoning*, *Contributions to Mineralogy and Petrology*, **142**, 436–448.
- GIORDANO D., RUSSEL J.K. and DINGWELL D.B. (2008), *Viscosity of magmatic liquids: a model*, *Earth and Planetary Sciences*, **271**, 123–134.
- HECHT, L. and VIGNERESSE, J.L. (1999), *A multidisciplinary approach combining geochemical, gravity and structural data: implications for pluton emplacement and zonation*, *Geological Society, London, Special Publications*, **168**, 95–110.
- HUPPERT, H.E. (2000), *Geological fluid mechanics, Perspectives in Fluid Dynamics. A collective introduction to current research*. G.K. Batchelor, H.K. Moffat and M.G. Worster Ed. (Cambridge University Press), 447–506.

- JANA, S.C., METCALFE, G., OTTINO, J.M. (1994), *Experimental and computational studies of mixing in complex Stokes flows: the vortex mixing flow and multicellular cavity flows*, J. Fluid Mech., 269, 199–246.
- KRIEGER, I. and DOUGHERTY, T. (1959), *A mechanism for non-Newtonian flow in suspension of rigid spheres*, Trans. Soc. Rheol., 3, 137–152.
- LE GUER, Y., EL OMARI K. (2012), Chaotic advection for thermal mixing, *Advances in Applied Mechanics*. In: E. van der Giessen and H. Aref Series Ed. Guest Ed. H.J.H. Clercx and M.F.M. Speetjens (San Diego: Academic), 45, 189–237.
- LEFEVRE, A. and MOTA, J.P.B. and RODRIGO, A.J.S. and SAATDJIAN, E. (2003), *Chaotic advection and heat transfer enhancement in Stokes flows*, International Journal of Heat and Fluid Flow, 24(3), 310–321.
- LIU, W., HALLER, G. (2004), *Strange eigenmodes and decay of variance in the mixing of diffusive tracers*, Physica D, 188, 1–39.
- LIU, M., PESKIN, R.L., MUZZIO, F.J. and LEONG, C.W. (1994), *Structure of the stretching field in chaotic cavity flows*, AIChE Journal, 40(8), 1273–1286.
- LOPEZ, C., NEUFELD, Z., HERNANDEZ-GARCIA, E. and HAYNES, P.H. (2001), *Chaotic advection of reacting substances: Plankton dynamics on a meandering jet*, Physics and Chemistry of the Earth, Part B: Hydrology, Oceans and Atmosphere, 26, 4, 313–317.
- MADER, H.M., LLEWELIN E.W., MUELLER, S.P. (2013), *The rheology of two-phase magmas: A review and analysis*, Journal of Volcanology and Geothermal Research, 257, 135–158.
- MAHOOD, G., and FRIDRICH, C., 1982, *Differentiation in waxing and waning magma chambers (abs.)*, Geological Society of America Abstracts with Programs, 14, 7, 553–554.
- MARSH, B.D. (1981), *On the crystallinity, probability of occurrence and rheology of lava and magma*, Contrib. Mineral. Petrol., 78, 85–98.
- MC BIRNEY, A.R. and MURASE, T. (1984), *Rheological properties of magmas*, Ann. Rev. Earth Planet. Sci. 12, 337–357.
- METCALFE, G., BINA, C.R. and OTTINO J.M. (1995), *Kinematic considerations for mantle mixing*, Geophys. Res. Lett. 22(7), 743–746.
- MORGAVI D., PERUGINI, D., DE CAMPOS, C.P., ERTEL-INGRISCH, W., LAVALLÉE, Y., MORGAN, L. and DINGWELL, D.B. (2013), *Interactions between rhyolitic and basaltic melts unraveled by chaotic mixing experiments*, Chemical Geology, 346, 199–212.
- MOTA, J.P.B., RODRIGO, A.J.S., SAATDJIAN, E. (2007), *Optimization of heat-transfer rate into time-periodic two-dimensional Stokes flows*, International Journal for Numerical Methods in Fluids, 53(6), 915–931.
- OTTINO, J.M., *The Kinematics of Mixing: Stretching, Chaos and Transport* (Cambridge University Press, Cambridge 1989).
- PERUGINI D., DE CAMPOS, C.P., ERTEL-INGRISCH, W. and DINGWELL, D.B. (2012), *The space and time complexity of chaotic mixing in silicate melts: implications for igneous petrology*, Lithos, 155, 326–340.
- PERUGINI, D., DE CAMPOS, C.P., DINGWELL, D.B. and DORFMAN, A. (2012), *Relaxation of concentration variance: A new tool to measure chemical element mobility during mixing of magmas*, Chemical Geology, 335, 8–23.
- PERUGINI, D., PETRELLI, M., POLI, G. (2006), *Diffusive fractionation of trace elements by chaotic mixing of magmas*, Earth Planet. Sci. Lett., 243, 669–680.
- PERUGINI, D., POLI, G. and VALENTINI, L. (2005), *Strange attractors in plagioclase oscillatory zoning: petrological implications*, Contributions to Mineralogy and Petrology, 149(4), 482–497.
- PERUGINI, D. and POLI, G. (2012), *The mixing of magmas in plutonic and volcanic environments: Analogies and differences*, Lithos, 153, 261–277.
- PERUGINI, D. and POLI, G., (2000), *Chaotic dynamics and fractals in magmatic interaction processes: a different approach to the interpretation of mafic microgranular enclaves*, Earth Planet. Sci. Lett., 175, 93–103.
- PERUGINI, D. and VALENTINI, L. and POLI, G. (2007), *Insights into magma chamber processes from the analysis of size distribution of enclaves in lava flows: A case study from Vulcano Island (Southern Italy)*, Journal of Volcanology and Geothermal Research, 166, 193–203.
- PERUGINI D., POLI G., MAZZUOLI R. (2003), *Chaotic advection, fractals and diffusion during mixing of magmas: evidence from lava flows*, J. Volc. Geotherm. Res., 2615:1–25.
- PETRELLI, M., PERUGINI, D., POLI, G. (2011), *Transition to chaos and implications for time-scales of magma hybridization during mixing processes in magma chambers*, Lithos, 125(1–2), 211–220.
- PIKOVSKY, A., POPOVYCH, O. (2003), *Persistent patterns in deterministic mixing flows*, Europhys. Lett., 61(5):625–631.
- RENJITH, M.L., CHARAN, S.N., SUBBARAO, D.V., BABU, E.V.S.S.K. and RAJASHEKHAR, V.B. (2013), *Grain to outcrop-scale frozen moments of dynamic magma mixing in the syenite magma chamber, Yelagiri Alkaline Complex, South India*, Geoscience Frontiers, in press, 1–20.
- ROSCOE, R. (1952) *The viscosity of suspensions of rigid spheres*, British Journal of Applied Physics, 3, 267–269.
- ROTHSTEIN, D., HENRY, E., and GOLLUB, J.P. (1999), *Persistent patterns in transient chaotic fluid mixing*, Nature, 401:770–772.
- SAATDJIAN, E. and LEPREVOST, J.C. (1998), *Chaotic heat transfer in a periodic two-dimensional flow*, Physics of Fluids, 10, 8, 2102–2104.
- SATO, H. (2005), *Viscosity measurement of subliquidus magmas: 1707 basalt of Fuji volcano*, Journal of Mineralogical and Petrological Sciences, 100, 133–142.
- SPERA, F.J. (2000), *Physical Properties of Magma*, in: Sigurdsson, H. (Ed.), Encyclopedia of Volcanoes. Academic Press, San Diego, CA, 171–189, 2000.
- STREMLER, M.A. (2008), *Mixing measures*, Encyclopedia of Microfluidics and Nanofluidics (ed. Li D., New York, Springer), 1376–82.
- THIFFEAULT, J.-L. (2012), *Using multiscale norms to quantify mixing and transport*, Nonlinearity 25, 1–44.
- WINKLER, H.G.F. (1949), *Crystallization of basaltic magma as recorded by variation of crystal-size in dikes*, Mineral. Mag., 28, 557–574.